Specific interaction to PIP$_2$ increases the kinetic rate of membrane binding of VILIPs, a subfamily of Neuronal Calcium Sensors (NCS) proteins

CrossMark

Samuel Rebaud [a], Conan K. Wang [b], Joe Sarkis [a], Lyndel Mason [b], Anne Simon [a], Loïc J. Blum [a], Andreas Hofmann [b,c], Agnès P. Girard-Egrot [a,*]

[a] Institut de Chimie et Biochimie Moléculaires et Supramoléculaires, Université Lyon 1, University of Lyon, ICBMS, CNRS UMR 5246, Bât. Curien, 43 bd du 11 Nov. 1918, F-69622 Villeurbanne cedex, France
[b] Structural Chemistry Program, Eskitis Institute for Cell and Molecular Therapies, Griffith University, Brisbane Qld 4111, Australia
[c] Faculty of Veterinary Science, The University of Melbourne, Parkville, Victoria, Australia

ARTICLE INFO

ABSTRACT

VIsinin-LIke Proteins (VILIPs) are a subfamily of the Neuronal Calcium Sensor (NCS) proteins, which possess both N-myristoylation and EF-hand motifs allowing for a putative 'calcium–myristoyl switch' regulation mechanism. It has previously been established that myristoyl conjugation increases the affinity of proteins for membranes, but, in many cases, a second feature such as a cluster of positively-charged residues is needed for stable membrane binding. The interaction of two members of this family, VILIP-1 and VILIP-3, with Langmuir monolayers as membrane models has been investigated in order to study the effects of both myristoylation and the highly basic region containing conserved poly-lysine residues on membrane association kinetics and binding properties. Results show that in the presence of calcium, N-myristoylation significantly increases the kinetic rate of VILIP adsorption to the membrane. Additionally, the proteins bind to negatively charged phospholipids independently of the conjugated myristate moiety. Besides the regulatory effect of calcium on the rate of binding presumably due to exposure of the myristoyl moiety ascribed to their putative 'calcium–myristoyl switch', VILIP-1 and -3 also engage specific interactions with biomimetic membranes containing phosphatidylinositol 4,5-bisphosphate (PIP$_2$). The presence of PIP$_2$ increases the membrane association rates of both VILIPs. Taken together, these results show the major kinetic role of N-myristoylation for membrane binding, and highlight the critical role of specific phosphoinositide interactions for membrane association of members of the VILIP family.

© 2014 Elsevier B.V. All rights reserved.

1. Introduction

VIsinin-LIke Proteins (VILIPs) are myristoylated proteins belonging to the family of the Neuronal Calcium Sensor (NCS) proteins, and their membrane binding capacity is thought to be regulated by a putative 'calcium–myristoyl switch' [1–3].

Lipid modifications of proteins play many roles inside and outside the cell [4]. They facilitate membrane attachment of soluble proteins by enhancing interactions of proteins with either organelle or plasma membranes, occur in signaling and subcellular targeting by directing proteins to various cellular membranes, promote intra- and intermolecular protein–protein interactions, and may modulate protein structure and function [5–10].

N-myristoylation of proteins has been identified as an essential regulatory component of signal transduction networks in many eukaryotic cells [7,11,12]. It comprises the covalent attachment of the 14-carbon saturated fatty acid myristate to the N-terminal glycine through a stable amide bond. One of the major functions of this fatty acid acylation is to promote membrane binding of a wide variety of proteins by simple insertion of hydrophobic myristate moiety into the lipid bilayer [9,12–15]. The covalent attachment of myristate to a protein results in increased hydrophobicity of the protein, leading to higher membrane binding affinity [4]. However, the increase in hydrophobicity is modest and often reversible membrane binding is observed. A central tenet, originally established by Peitzsch and McLaughlin [16] is that the effective dissociation constant K_d (approximately 10^{-4} M) of membrane-bound myristoylated peptides corresponds to an energy just enough for attachment of the peptides to the membrane. It is now an established paradigm that myristoylation, although necessary for membrane binding, is not sufficient to stably anchor a protein to a lipid bilayer [9]. Moreover, many myristoylated proteins require a second feature for stable membrane binding, like an additional domain that interacts

* Corresponding author at: Institut de Chimie et Biochimie Moléculaires et Supramoléculaires (ICBMS), Equipe GEMBAS, UMR CNRS 5246, Université Lyon 1, Bât Curien, 43 bd du 11 novembre 1918, 69622 Villeurbanne, France. Tel.: +33 4 72 44 85 32; fax: +33 4 72 44 79 70.
E-mail address: agnes.girard-egrot@univ-lyon1.fr (A.P. Girard-Egrot).

with another membrane-bound protein [9,15,17,18] or a cluster of positively-charged residues often localized in the vicinity of the myristoylation site of the protein [9,12,13,19]. Indeed, the N-terminal region of myristoylated proteins contains in many cases a polybasic region capable of electrostatic interactions with acidic phospholipid headgroups, mainly phosphatidylserine (PS) and phosphatidylinositol (PI) which, in healthy cells, are primarily localized to the inner leaflet of the bilayer, imparting a net negative charge to the cytoplasmic leaflet surface [20]. In addition, the occurrence of polybasic motif is now correlated with the targeting of plasma membrane proteins due to recognition of polyphosphoinositides, like PI(3,4,5)P$_3$ or PI(4,5)P$_2$ [21,22], that are highly charged (valence of -4 at pH 7.0 [23]). Specific interactions with PIPs may target plasma membrane proteins to distinct cellular signaling processes [24,25].

When both myristate and polybasic motif ('*myristate plus basic*' model) are present within the protein, the hydrophobic and electrostatic forces synergize [13], but mechanistic details of this synergy have not been reported to date. Functionally, protein lipid modifications can also act as reversible switches to activate or terminate signaling process. Indeed, the anchorage of *N*-myristoylated proteins to membranes may be dynamically regulated *via* various "myristoyl-switches". One of these switches relies on a "ligand"-dependent conformational change of the protein leading to exposure of the myristoyl moiety, previously sequestered in a hydrophobic pocket to outside, where it becomes available to participate in membrane binding. The switch can be triggered by binding of ligands or drugs, or by multimerization, thereby regulating the distribution of the myristoylated protein between cytosolic and membrane-bound states [9]. This concept is exemplified by the binding of calcium in the intramolecular '*calcium–myristoyl switch*' [4,6,26] where the transition of the conjugated myristoyl group from the buried to the exposed conformation is triggered by the binding of calcium cations to EF-hand motifs [26,27]. Proteins that are subject to a myristoyl switch typically exhibit a membrane binding regulation [28], but few mechanistic insights have been obtained to date.

The group of VIsinin-LIke Proteins (VILIPs) is comprised of VILIP-1, VILIP-2, VILIP-3, hippocalcin and neurocalcin δ [29]. These proteins are involved in many diseases such as Alzheimer's disease [19,30,31], schizophrenia [32,33] and cancer [34–36]. Previous studies have shown that VILIP-1 and VILIP-3 act at the membrane where they regulate the function of various membrane receptors like adenylate/guanylate cyclase, nicotinic acetylcholine receptor and natriuretic peptide receptor B [34,37–39]. Cell biological studies have shown that VILIPs translocate to membranes upon stimulation by elevated intracellular calcium levels where they are implicated in signal transduction [1,2,40]. However, at a molecular level, the mechanisms of membrane association are less clear. It has been established that members of the NCS family, including VILIPs, possess both an N-terminal myristoyl group and EF-hand structural motifs [29,41]. The combination of these two structural elements is an essential component of the membrane binding regulation by the way of a '*calcium–myristoyl switch*', which has been suggested for VILIPs [1,2,41,42], but only show without ambiguity for recoverin, the prototypic member of the NCS family [27,43]. Intriguingly, the subcellular membrane localization of VILIPs differs substantially in living cells [2,40], and may be due to their capability to specifically bind to phosphatidyl inosities, most likely mediated through several highly conserved lysine residues in the N-terminal region of VILIPs [22]. The existence of such a binding site has been supported by results from docking and molecular dynamics simulations [22]. Nonetheless, the mechanistic interplay between protein–membrane electrostatic interactions and the membrane insertion of the myristoyl moiety in the presence of calcium during the membrane binding process is not fully understood.

In this work, we investigated the interaction of VILIP-1 and VILIP-3 with membrane models using Langmuir monolayers and Brewster Angle Microscopy (BAM). These techniques have been previously used to investigate the contribution of the myristoyl group and hydrophobic

amino acids of recoverin to its binding dynamics [44] and the importance of polyunsaturated phospholipids which highly favor the binding of this protein [45]. Recently, it has been employed to evaluate the effect of membrane composition in terms of charge and acyl chain saturation on the membrane binding of VILIPs, showing that the proteins initially interact with the membrane through electrostatic interactions [46]. In the present study, we clearly show, by using myristoylated and unmyristoylated proteins, that the presence of calcium only increases the association kinetic rates of the myristoylated proteins with the membrane. We also demonstrate that membrane binding involves electrostatic interactions of the proteins with acidic phospholipid headgroups, and that the rate of binding is enhanced by the inclusion of PIP$_2$ into the membrane. We suggest that interactions of VILIPs with PIP$_2$, likely due to the presence of the polybasic region at the N-terminus, strengthens the association of VILIPs with the membrane and assists conformational changes in the protein triggered by the binding of calcium in the EF-hand sites, which accelerates the binding of VILIPs into membranes. These results reveal the major kinetic role of the N-myristoylation for the binding to the membrane, and highlight an important mechanistic role of phosphoinositides for membrane association of members of the VILIP family.

2. Material and methods

2.1. Chemicals

Ultrapure water was obtained from a PURELAB option Q7 system (VEOLIA WATER STI, France). Its resistivity and surface tension were 18.2 MΩ.cm and 72.8 mN/m at 20 °C, respectively. 4-(2-Hydroxyethyl)-1-Piperazine ethane sulfonic acid (HEPES), sodium chloride (NaCl), calcium chloride (CaCl$_2$) and Ethylenediamine tetra-acetic acid (EDTA) were purchased from Sigma (Saint-Quentin Fallavier, France). 1,2-dioleoyl-*sn*-glycero-3-phosphocholine (DOPC), 1,2-dioleoyl-*sn*-glycero-3-phosphoserine (DMPS), 1,2-dimyristoyl-*sn*-glycero-3-phosphocholine (DMPC), 1,2-dimyristoyl-*sn*-glycero-3-phosphoserine (DMPS) and 1,2-dioleoyl-*sn*-glycero-3-phosphoinositol-4,5-bisphosphate (PI(4,5)P$_2$) were purchased from Avanti Polar Lipids (Alabaster, AL, USA). All chemicals were used as received. The phospholipid solutions were prepared in chloroform at a concentration of 1 mg/mL and stored at -20 °C under argon to prevent lipid oxidation [47].

2.2. Preparation of recombinant VILIP-1 & VILIP-3

The recombinant wild-type proteins were produced as previously described [41]. Briefly, VILIP-1 (ligated into pET8c [48]) and VILIP-3 (ligated into pRSET_C) were expressed in BL21(DE3) cells, which in case of myristoylated VILIPs, were co-transformed with either of the above VILIP expression plasmids as well as N-myristoyl transferase (NMT; plasmid pBB131). Recombinant proteins were purified by subsequent anion exchange chromatography (QA52 column), and hydrophobic interaction chromatography, using a phenyl sepharose column. The purified proteins were stored in buffer containing 20 mM HEPES, 100 mM NaCl, pH 7.4, at a final concentration close to 1 mg/mL. Protein quality was monitored using denaturing SDS-PAGE and mass spectrometry.

2.3. Langmuir monolayer experiments

Monolayers were prepared using a homemade rectangular Langmuir PTFE-trough with a symmetrical compression system. The rectangular trough had a volume of 25 mL and a surface area of 49 cm^2. A Wilhelmy balance was used to measure the surface pressure (π), with an accuracy of ± 0.5 mN/m. The trough was cleaned with successive baths of dichloromethane, ethanol and water, and filled with a filtered 20 mM HEPES buffer (pH 7.4), 150 mM NaCl, containing either 2 mM CaCl$_2$ or 2 mM EDTA. The subphase buffer was maintained at 20 °C

during all the experiments. Phospholipid mixture solutions in chloroform were gently spread at the air/liquid interface of the HEPES buffer subphase. After 15 min allowing solvent evaporation, the monolayer was compressed by the two mobile barriers until the desired surface pressures ranging from 5 to 20 mN/m and corresponding to the initial surface pressures (π_i). The protein was then injected into the subphase just beneath the lipid monolayer at a final concentration of 30 nM. The surface pressure variation induced by the interaction of the protein with the monolayer was continuously recorded as a function of time by using a computer-controlled Langmuir film balance (KSV NIMA) until the equilibrium surface pressure (π_e) was reached, indicating the end of the adsorption kinetics. All measurements were repeated at least three times for each condition and the average values were reported in this study.

2.4. Adsorption kinetics of VILIPs

The surface pressure increase ($\Delta\pi$ in mN/m) after injection of the proteins corresponded to $\pi_e - \pi_i$. The curves of surface pressure increase ($\Delta\pi$) as a function of time (t) recorded during the adsorption of VILIPs onto phospholipid monolayers corresponded to the adsorption kinetics of the protein. They were fitted using the stretched exponential equation adapted to surface pressure measurements by Pitcher et al. [49], $\pi_t = \pi_e - \pi_i e^{-(kt)\beta}$ where π_t is the surface pressure of the monolayer at time t, π_e is the final equilibrium surface pressure after protein adsorption, π_i is the initial surface pressure, k the rate coefficient of the binding of the protein onto the monolayer, and β is an exponential scaling factor.

2.5. Determination of the binding parameters of VILIPs

The different parameters that characterize the binding of VILIPs to different phospholipid membranes were determined as recently described [50,51]. Briefly, the plot of the surface pressure increases ($\Delta\pi$) as a function of different initial surface pressures π_i allowed the determination of three different parameters: the Maximum Insertion Pressure (MIP) and the $\Delta\pi_0$ by extrapolating the regression of the plot to x and y axes, respectively; and the synergy factor (a) which is obtained by adding 1 to the slope of the plot of $\Delta\pi$ as a function of π_i [51]. The uncertainty was determined as previously described [50]. In this study, and because the parameter $\Delta\pi_0$ is more difficult to describe and still a point of debate [50], only MIP and (a) values will be presented.

2.6. Brewster angle microscopy

Brewster Angle Microscopy (BAM) allows the characterization of the lipid domain morphology of monolayers at the air/water interface [52]. The phospholipid morphology before and after protein injection was determined using a Brewster angle microscope EP³SW (Accurion, Germany) equipped with a 532 nm laser, a polarizer, an analyzer and a CCD camera. BAM image size was 483 × 383 μm.

For ultrathin films, the reflectance depends on both thickness and refractive index of the monolayer. Fitting reflectance data with BAM modeling software leads to a deduction of film thickness for a given refractive index. This model is based on the proportional relationship between the reflectance and the square of the interfacial film thickness when the optical index of the film is assumed constant [53–55]. According to Winsel et al. [54], a reasonable range of the refractive index for biological materials is comprised between 1.43 and 1.47. Since it was difficult to determine an accurate experimental refractive index value for mixed lipid-protein film, it is admitted to use the same average value of the refractive index 1.45 for both lipid layers and proteins in order to reduce the number of parameters introduced in the model [56–60]. The different views of the interfacial film were reconstituted using BAM software EP³viewer (Accurion, Germany) based on the brightness of the BAM pictures.

3. Results

To examine the role of both the positively-charged region and the N-myristoylation in the presence of calcium as putative 'calcium–myristoyl switch' mechanism in the sequential events of the binding of VILIPs to membranes, we explored the membrane binding properties of four different proteins, VILIP-1 and VILIP-3 in their myristoylated and non-myristoylated forms, by using reconstituted monolayers at an air/liquid interface (Langmuir monolayers). Before characterization of binding, we investigated the interfacial behavior of each protein at the air/liquid interface in the absence of lipids in order to determine the optimal protein concentration to inject into the subphase for subsequent protein/lipid interaction analysis.

3.1. Adsorption of VILIPs at an air/liquid interface

Experiments without lipid at an air/liquid interface allow for the determination of: i) the tensio-active properties of the protein; ii) the concentration at which the protein saturates the lipid-free interface in order to minimize the protein aggregation that could result from a high protein concentration [61,62]; and iii) the concentration that will be used in the experiments with lipids. Consensually, the protein concentration is chosen based on these pre-valuations is lower than the saturation concentration [57].

The adsorption of recombinant protein at varying subphase concentrations in the range of 3.75–30 nM was monitored by surface pressure measurements. At each concentration, the surface pressure equilibrated to a value indicating the end of the adsorption kinetics; this value indicates the equilibrium adsorption surface pressure (π_e). A typical relationship between π_e and the final protein concentration injected into the subphase containing 2 mM of CaCl$_2$ is shown in Fig. 1A. For each protein, π_e values increased in a concentration dependent manner up to a saturation value. Depending on the individual protein, saturation levels were reached at a protein concentration of 15 or 30 nM (data not shown). At 30 nM, we found that myristoylated VILIP-1 and -3 possessed higher equilibrium adsorption surface pressures than the non-myristoylated proteins (Fig. 1A — Inset). After injection of myristoylated VILIP-1 and VILIP-3 into the subphase and equilibration of the surface pressure (π_e), BAM images were recorded in order to visualize the film homogeneity and to determine the estimated thickness of the protein monolayer from the calibrated reflectance values. These images (Fig. 1B) revealed that at a concentration of 30 nM, proteins formed a homogeneous interfacial film without any aggregation, and that the estimated thickness of the protein monolayers was about 2.26 ± 0.23 nm and 2.58 ± 0.27 nm for myristoylated VILIP-1 and VILIP-3, respectively.

Since myristoylated VILIPs did not form aggregates under the chosen conditions, protein–lipid interactions can be investigated at 30 nM protein concentration at the lipid/liquid interface.

Fig. 2 shows the adsorption kinetics of VILIP-1 in the presence or in the absence of calcium at the air–liquid interface at a final concentration of 30 nM. The difference in the adsorption surface pressure (π_e), although small, is significant. It could be ascribed to an increase in the hydrophobicity of the protein in the presence of calcium. Furthermore, the same adsorption surface pressure (π_e) was reached if calcium was absent from the subphase or if the myristoyl moiety was removed from the protein (non-myristoylated form). This result was in favor of a probable exposure of the myristoyl group due to the presence of calcium which arrests the protein at a naked air–liquid interface.

3.2. In the presence of calcium, N-myristoylation accelerates the binding of VILIPs to membranes

Next we investigated the membrane binding properties of myristoylated and unmyristoylated VILIP-1 and -3 using reconstituted monolayers at an air/liquid interface, in the presence or in the absence of calcium ions. Langmuir phospholipid monolayer films have become
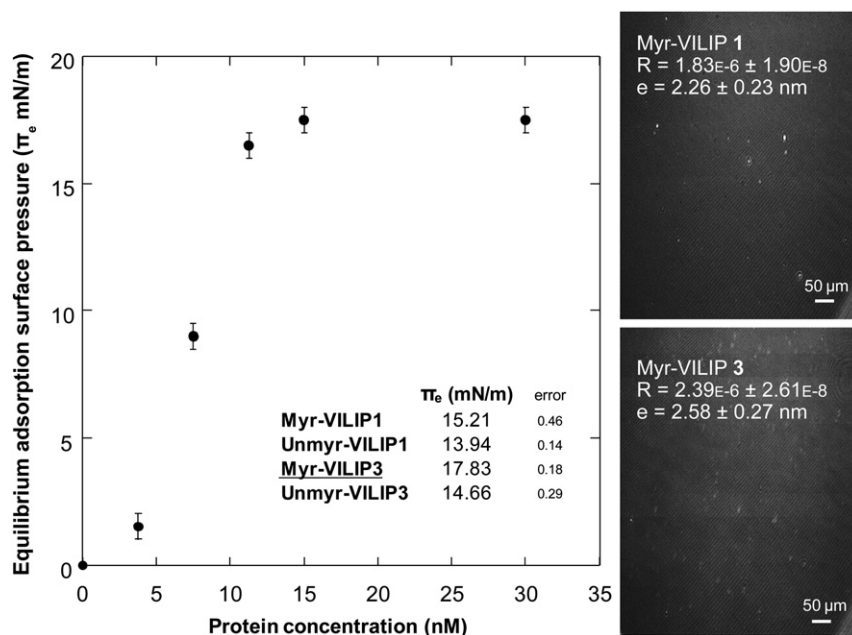
Myr-VILIP **1**
R = 1.83E-6 ± 1.90E-8
e = 2.26 ± 0.23 nm

50 µm

Myr-VILIP **3**
R = 2.39E-6 ± 2.61E-8
e = 2.58 ± 0.27 nm

50 µm

	π_e (mN/m)	error
Myr-VILIP1	15.21	0.46
Unmyr-VILIP1	13.94	0.14
Myr-VILIP3	17.83	0.18
Unmyr-VILIP3	14.66	0.29

Fig. 1. Adsorption of protein at an air/liquid interface. (A) Typical curve of the equilibrium adsorption surface pressure (π_e) reached at the end of the adsorption kinetics for different protein concentration injected into the subphase. Each point corresponds to the mean value of three kinetic experiments. (Inset) values of (π_e) for each protein at 30 nM. (B) BAM images at equilibrium surface pressure after injection of myr-VILIP1 or myr-VILIP3 at a final concentration of 30 nM, with corresponding reflectance and estimated thickness for a reflective index value of 1.45. Subphase: 20 mM HEPES 150 mM NaCl 2 mM CaCl$_2$.

a standard model for studying lipid–protein interactions and they serve as mimics of biological membranes to study protein–membrane association [46,51,60,63–65]. As electrostatic interactions are believed to be involved in the association of VILIPs to membranes [41,46], phospholipid monolayers composed of negatively charged (PS) and neutral lipids (PC) were used; both types of phospholipids are components of the inner leaflet of the plasma membrane.

The monolayers were compressed to an initial surface pressure (π_i) of 15 mN/m. Upon injection of protein into the subphase, the surface pressure variation ($\Delta\pi$ in mN/m) was recorded as a function of time, and the adsorption kinetics were fitted to the Pitcher's equation to determine the rate of binding k (Fig. 2) [49,50]. The final surface pressure
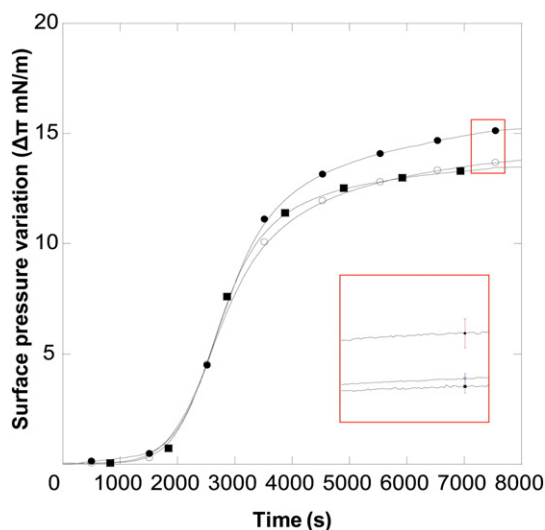

Fig. 2. Adsorption kinetics of VILIPs in the presence or in the absence of calcium at the air–liquid interface for a final concentration of 30 nM. Representative surface pressure variation as a function of time for myristoylated (circle) or unmyristoylated (square) VILIP-1 injected into the buffer. The curves render during adsorption of the protein at the air–liquid interface in the presence of 2 mM CaCl$_2$ (black) or 2 mM EDTA (white).

variations ($\Delta\pi$ in mN/m) were independent of the presence or absence of calcium (Fig. 3A). However, the maximum $\Delta\pi$ values were lower for the unmyristoylated compared to the myristoylated proteins. The absence or presence of calcium did not alter the kinetic curves for the unmyristoylated proteins, but caused slight differences for the myristoylated proteins.

The capacity of unmyristoylated proteins to interact with the biomimetic membrane indicates the existence of another binding site distinct from the conjugated lipid group. Nevertheless, the highest final values of $\Delta\pi$ were obtained for the myristoylated proteins emphasizing the role of this lipo-conjugate in VILIP membrane association by either strengthening the protein binding to the membrane or anchoring more protein molecules to the membrane. Intriguingly, this effect elicited by the myristoyl group is independent of the presence of calcium since the same $\Delta\pi$ values were obtained with or without calcium for both myristoylated proteins at the end of the adsorption process (after ~50 min). The presence of calcium did not seem to affect the final affinity of VILIPs for membranes.

The second parameter characterizing monolayer adsorption kinetics is the rate of binding "k". Determination of this parameter is possible by fitting the kinetic curve to the Pitcher's equation. It allows discrimination between different protein behaviors, when similar $\Delta\pi$ is observed [50].

In the case of VILIPs, a clear effect of calcium was observed on the rate of binding k of the myristoylated proteins (Fig. 3B). In the presence of calcium, we observed an increase of 53% and 135% of the k value for myristoylated VILIP-1 and VILIP-3 respectively, compared to the values obtained in the presence of EDTA. This effect was not observed for the unmyristoylated proteins. One explanation for these observations is that the myristoyl moiety could be more rapidly available to interact with the monolayer in the presence of Ca^{2+}. Without N-myristoylation, calcium has no effect on the kinetics. Intriguingly, the values of k determined for myristoylated proteins in the absence of calcium were equal to those obtained for the unmyristoylated proteins in the presence or absence of calcium (Fig. 3B). This suggests that binding involves another site, which is consistent with the existence of electrostatic interactions between VILIP-1 and -3, and the surface of membrane, as previously shown [41,46].
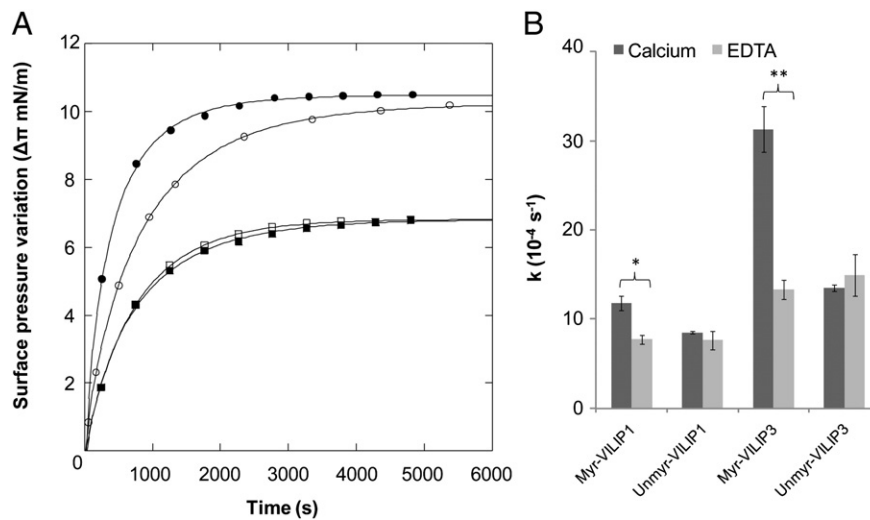
Fig. 3. Adsorption kinetics of VILIPs onto DOPC/DOPS (1:3) phospholipid monolayers. (A) Representative surface pressure variation as a function of time for myristoylated (circle) or unmyristoylated (square) VILIP-3 injected underneath the monolayer initially compressed at an initial surface pressure (π_i) of 15 mN/m. The curves render during adsorption of the protein in the presence of 2 mM CaCl$_2$ (black) or 2 mM EDTA (white). All kinetics are fitted to the Pitcher's equation which allowed the determination of the rate of binding (k). The same variation profile has been obtained with VILIP-1. (B) Rate of binding for VILIP-1 and VILIP-3 (*p < 0.05; **p < 0.01).

In summary, these results show that a part of the binding kinetics is independent of the presence of the myristoyl moiety. However, in the presence of calcium, it appears that the N-myristoylation accelerates binding of VILIPs to membranes. The kinetics is much faster than that of the non-myristoylated form. This last result is consistent with that previously reported for recoverin [45].

3.3. Effect of the myristoyl group on VILIP membrane binding properties

To further characterize the effects of the myristoyl group on the interaction of VILIPs with membranes, we monitored the surface pressure ($\Delta\pi$) after injection of the protein underneath the compressed monolayer with varying initial surface pressure (π_i), ranging from 5 to 20 mN/m (Fig. 4). Such correlations are frequently analyzed to assess lipid–protein interactions and to distinguish electrostatic and hydrophobic interactions [60,62,63,66,67].

As shown in Fig. 4A and B, the maximum insertion pressure (MIP) was significantly higher for myristoylated VILIP-1 and -3 than their unmyristoylated forms. In the presence of 2 mM CaCl$_2$, MIP values for VILIP-1 were 23.7 $\pm$ 2.8 mN/m and 18.6 $\pm$ 1.1 mN/m, respectively (Fig. 4A). In the presence of 2 mM EDTA, MIP values were 22.7 $\pm$ 1.4 mN/m and 19.5 $\pm$ 1.5 mN/m. For myristoylated and unmyristoylated VILIP-3 (Fig. 4B) MIP values of 26.6 $\pm$ 0.5 mN/m and 15.5 $\pm$ 0.8 mN/m were obtained in presence of 2 mM CaCl$_2$. In the presence of 2 mM EDTA, MIP values were 24.4 $\pm$ 1.4 mN/m and 17.1 $\pm$ 3.4 mN/m. These results are in agreement with our previous conclusions on the role of
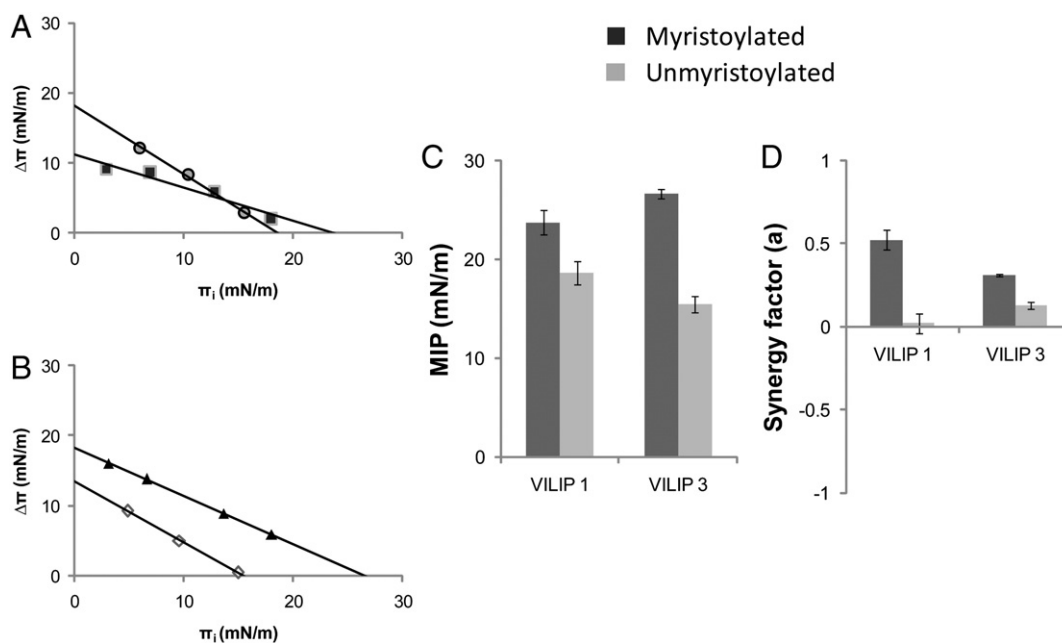

Fig. 4. Determination of the maximal insertion pressure (MIP) and synergy factor (a) of VILIPs. (Left) Plot of the surface pressure increase ($\Delta\pi$) as a function of the initial surface pressure (π_i) to determine the MIP and the synergy factor (a) for myristoylated (square) and unmyristoylated (circle) VILIP-1 (A) and for myristoylated (triangle) and unmyristoylated (diamond) VILIP-3 (B) in interaction with a DOPC/DOPS (3:1) phospholipid monolayer. The subphase was supplemented by 2 mM CaCl$_2$. (Right) Histograms of MIP(C) and synergy factor (a) (D) for VILIPs in the presence of calcium. Same results and effects have been obtained in the absence of calcium (data not shown).

the N-myristoylation (see above). In the presence of calcium, the highest MIP values obtained for the myristoylated proteins demonstrate the membrane anchoring effect of the myristoyl group (Fig. 4C). In contrast, removal of the myristate decreases the membrane affinity. However, MIPs determined for both myristoylated proteins in the absence of calcium were similar to those obtained in the presence of the cation. No effect was observed on the final association of the proteins to the membrane. When the myristoylated proteins are already in contact with the monolayer, the calcium no longer has an effect on the extent of binding. The phenomenon was not observed in the absence of lipid at the air–liquid interface (Fig. 2).

It has been previously shown by Salesse's group [50] that the synergy factor "a" can deliver insights into mechanisms governing protein binding to lipid monolayers. A positive a value indicates favorable conditions for protein monolayer binding. A synergy factor of zero corresponds to a stationary state, without any favored or disfavored protein membrane binding. Finally, a negative synergy factor indicates repulsion between the protein and the monolayer. Here, our data yield synergy factors with substantially positive values for myristoylated proteins ($a = 0.522 \pm 0.059$ for myristoylated VILIP-1 and 0.312 ± 0.007 for myristoylated VILIP-3), and around zero for the unmyristoylated proteins (Fig. 4D). These values agree with the notion that the presence of the myristoyl group facilitates the association of VILIPs to the monolayer. In the absence of N-myristoylation, the membrane binding properties of VILIPs are markedly less sensitive to the compaction of the lipid in the monolayer. Since the synergy factor is a measure of the sensitivity for the packing of phospholipid acyl chains, the insertion of the myristoyl group within the monolayer is favored by the hydrophobic chain organization. Membrane binding becomes insensitive to the acyl chain organization when it is only mediated by surface electrostatic interactions.

3.4. VILIPs bind to negatively charged phospholipids

In order to assess the potential organizational changes within the monolayer upon lipid/protein interactions, Brewster angle microscopy (BAM) was used to scrutinize the morphologies of phospholipid monolayers. As shown in Fig. 5 (top line), DOPC/DOPS (1:3) monolayers are homogenous irrespective of the surface pressures applied. By using BAM calibration procedure and thickness model [53,57], an estimated thickness of 1.4 nm was determined from true reflectance values for pure lipid monolayers compressed at 15 or 25 mN/m, respectively,

consistent with the thickness of one membrane leaflet in a fluid phase (Table 1). After injection of myristoylated VILIPs beneath monolayers compressed at π_i of 15 mN/m, and subsequent equilibration ($\pi_e = 21$ mN/m for myristoylated VILIP-1 and 25 mN/m for VILIP-3), the monolayers remained homogeneous (Fig. 5 — top line). The global estimated thickness of the film increased from 1.43 to 2.19 nm for myristoylated VILIP1, and from 1.43 to 2.56 nm for myristoylated VILIP-3, due to the interaction of these proteins with the fluid monolayer. The phase transition temperature of phospholipids can affect the occurrence of morphological changes in the membrane. Since 1,2-dioleyl-sn-glycero-3-phospholipids (DOPC and DOPS) remained in the fluid phase in the experimental conditions used in this study, we also tested 1,2-dimyristoyl-sn-glycero-3-phospholipids, DMPC and DMPS, which possess different phase transition temperatures to examine the effect of phospholipid reorganization upon interactions [63,67]. In the absence of protein, DMPC/DMPS (1:3) monolayers exhibited a classical phase segregation mediated by the presence of calcium in the subphase: the negatively-charged phospholipids DMPS segregated into condensed domains (bright clusters), while DMPC remained in the fluid phase (dark background) (Fig. 5 — bottom line). The estimated thickness of each phase was 2.37 nm and 1.79 nm, respectively, consistent with those expected for a condensed or a fluid phase (Table 1). In the presence of myristoylated VILIPs at equilibrium surface pressure, a drastic modification of the monolayer morphology was observed with a large rearrangement of the phospholipid organization compared to the pure monolayers at similar surface pressures. Although no significant change was detected in the estimated thicknesses upon injection (Table 1), in the condensed phase of DMPC/DMPS (1:3) bright dots appeared in the BAM images, especially in the presence of myristoylated VILIP-3 (Fig. 5 — Inset — red arrows). The film thickness in the area of these bright dots was determined to ~3.3 nm for both myristoylated VILIPs (Table 1). Although this thickness does not correspond to the sum of monolayer and protein thicknesses, one can assume that VILIPs may preferentially interact with the negatively charged condensed domains of PS. In line with this assumption are the results obtained with unmyristoylated VILIPs in this experiment (Fig. 5 and Table 1) which show the same membrane reorganization and estimated thicknesses.

Clearly, these effects are independent of the myristoylation state and thus due to other interactions between VILIPs and the membrane. The BAM images suggest that VILIPs bind to the negatively charged phospholipids, suggesting that the basic residues in the N-terminal region of the proteins are involved in the association process.
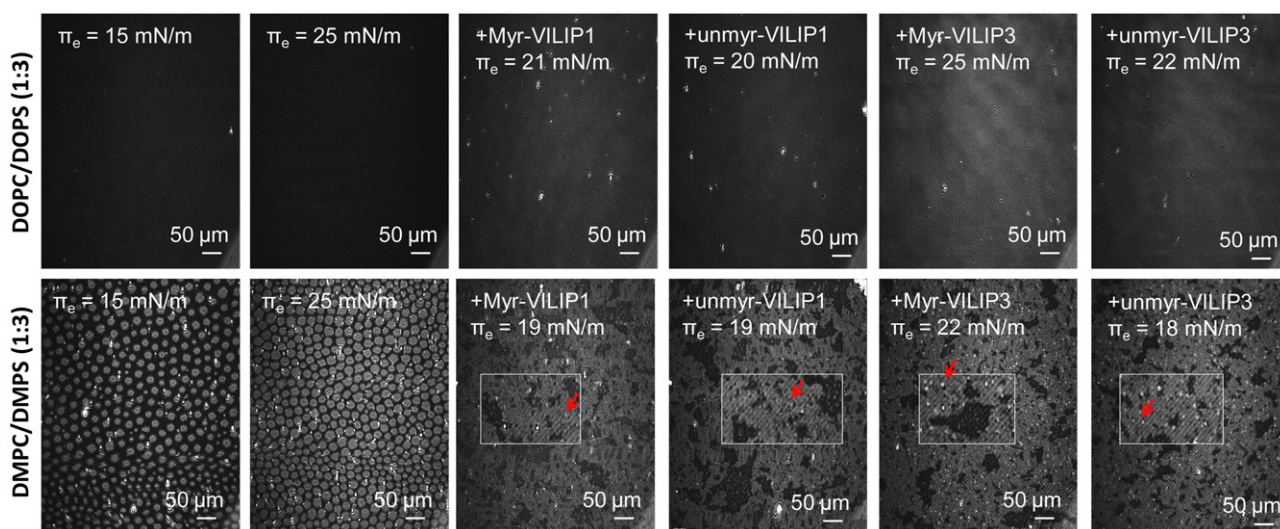

Fig. 5. Effects of the VILIPs adsorption on the lipid monolayer morphology. Interface visualization using Brewster angle microscopy of DOPC/DOPS (1:3) (top line) or DMPC/DMPS (1:3) (bottom line) monolayer at 15 mN/m or 25 mN/m, and at π_e after injection of notified VILIPs ($\pi_i = 15$ mN/m). Red arrows indicated bright dots in condensed phase.

Table 1
Estimated thicknesses and reflectance values of the film present at air buffer interface. Thickness values were estimated using the reflectance value, for a refractive index value of 1.45.

Lipids composition	Phase	Estimated thickness (nm) — reflectance					
		Lipid monolayer		Lipid monolayer in interaction with			
		15 mN/m	25 mN/m	Myr-VILIP1	unmyr-VILIP1	Myr-VILIP3	unmyr-VILIP3
DOPC/DOPS (1:3)	Fluid	1.43 ± 0.15 $0.74E^{-6} \pm 0.76E^{-8}$	1.46 ± 0.15 $0.77E^{-6} \pm 0.57E^{-8}$	2.19 ± 0.20 $1.72E^{-6} \pm 1.48E^{-8}$	1.94 ± 0.20 $1.35E^{-6} \pm 1.41E^{-8}$	2.56 ± 0.26 $2.35E^{-6} \pm 2.62E^{-8}$	1.93 ± 0.20 $1.34E^{-6} \pm 1.40E^{-8}$
DMPC/DMPS (1:3)	Fluid	1.81 ± 0.18 $1.18E^{-6} \pm 1.27E^{-8}$	1.79 ± 0.18 $1.15E^{-6} \pm 1.21E^{-8}$	1.83 ± 0.19 $1.21E^{-6} \pm 1.31E^{-8}$	1.69 ± 0.17 $1.03E^{-6} \pm 0.98E^{-8}$	1.81 ± 0.18 $1.18E^{-6} \pm 0.98E^{-8}$	1.80 ± 0.18 $1.16E^{-6} \pm 1.23E^{-8}$
	Condensed	2.39 ± 0.24 $2.05E^{-6} \pm 2.12E^{-8}$	2.37 ± 0.24 $2.02E^{-6} \pm 2.05E^{-8}$	2.43 ± 0.25 $1.97E^{-6} \pm 2.22E^{-8}$	2.52 ± 0.26 $2.29E^{-6} \pm 2.44E^{-8}$	2.46 ± 0.25 $2.17E^{-6} \pm 2.31E^{-8}$	2.50 ± 0.25 $2.24E^{-6} \pm 2.39E^{-8}$
	Bright dots (condensed)			**3.17 ± 0.32** $3.61E^{-6} \pm 3.60E^{-8}$	**3.36 ± 0.34** $4.06E^{-6} \pm 4.15E^{-8}$	**3.31 ± 0.33** $3.94E^{-6} \pm 3.82E^{-8}$	**3.38 ± 0.34** $4.10E^{-6} \pm 4.18E^{-8}$

3.5. Phosphoinositides enhance membrane interaction of VILIPs

It has been suggested that VILIPs can bind to phosphoinositol derivatives such as $PI(4,5)P_2$ [22]. In order to investigate potential effects of phosphoinositides on the adsorption kinetics of VILIPs, we conducted time-dependent adsorption experiments to DMPC/DMPS (1:3) monolayers containing 1% PIP_2 while maintaining a constant net negative charge on the monolayer surface. The exact composition of the monolayer was thus DMPC 25%, DMPS 74%, PIP_2 1%. No particular change was observed either for the morphology (Fig. 6A) or the estimated thickness (data not shown) of the films in the presence of myristoylated VILIPs when compared to a DMPC/DMPS (1:3) monolayer without proteins. Similarly, no major differences were observed at the end of the adsorption process: PIP_2 did not induce significant variations of the final surface pressure increase (Δπ values) upon VILIPs interaction (Fig. 6B). In contrast, a significant effect was observed for the values of the rate of binding k (Fig. 6C). Despite the net negative charge being the same in the monolayers with and without 1% PIP_2, the binding rate of all proteins was significantly increased in the presence of PIP_2 (30% increase in the case of the myristoylated proteins).

These results are in agreement with the suggestion that VILIPs can interact specifically with phosphoinositides and demonstrate that the main effect of PIP-containing membranes is of a kinetic nature. Again, since this increase was observed for myristoylated and unmyristoylated proteins in this study, we can assume that this specific interaction is independent of lipo-conjugation of VILIPs and most likely localizes to the binding site identified in previous modeling/molecular dynamics experiments [22]. It is consistent with the fact that any protein with a cluster of four or more basic residues located at the membrane-solution interface should laterally sequester PIP_2 [68]. Importantly, specific interactions of VILIPs with PIPs support the notion of PIP-targeting by VILIPs as a way to regulate its subcellular location.

4. Discussion

VILIPs have been implied in signal transduction processes [34,37–39], since they translocate to the plasma membrane following a stimulus that provides elevated intracellular calcium concentration. This translocation is thought to rely on a putative intramolecular 'calcium–myristoyl switch' [1,2,40–42]. Moreover, a putative basic cluster of conserved poly-lysine residues in the N-terminal region of *N*-myristoylated VILIPs, could provide a potential site for binding specifically phosphoinositides, and more precisely PIP_2 [22], and thus provide a molecular mechanism for the different subcellular localizations of VILIPs in the living cells [2]. As mentioned in the introduction, the two-signal model 'myristate plus basic' is well known to mediate efficient membrane binding. However, the interrelationship between the electrostatic interactions mediated by the polybasic domain and the insertion of the myristoyl group in the membrane in presence of calcium during the binding, potentially regulated by a 'calcium–myristoyl switch' mechanism, has not been reported yet.

In this study, we have investigated the membrane binding properties of VILIP-1 and VILIP-3 by using Langmuir monolayers as membrane models which offer the possibility to analyze in detail the membrane binding kinetics. The choice of this system was based on its simple experimental design and its compatibility with monotopic protein insertion in the membrane. By using a set of myristoylated and non-myristoylated proteins, we demonstrated that a part of the kinetics of binding to PS-containing monolayer is likely controlled by electrostatic interactions. Interestingly, the rate of binding k is of the same order of magnitude for unmyristoylated proteins (with or without calcium) and myristoylated proteins in the absence of calcium, for which the myristoyl group is supposed to be buried. This result suggests that the interactions between VILIPs and negatively-charged membranes involve other structural features aside from the myristate, and corroborates with recent finding indicating that a certain amount of VILIP-1 localizes to the plasma membrane even in the absence of the myristoyl group [69]. Similar results have previously been obtained for the NADH-cytochrome b5 reductase, where the association with the membrane of the non-myristoylated form of the enzyme was not different from that of the natural, myristoylated form [70]. These interactions are most likely of electrostatic nature and presumably mediated by the conserved basic residues found on the surface of VILIPs in the N-terminal region [41].
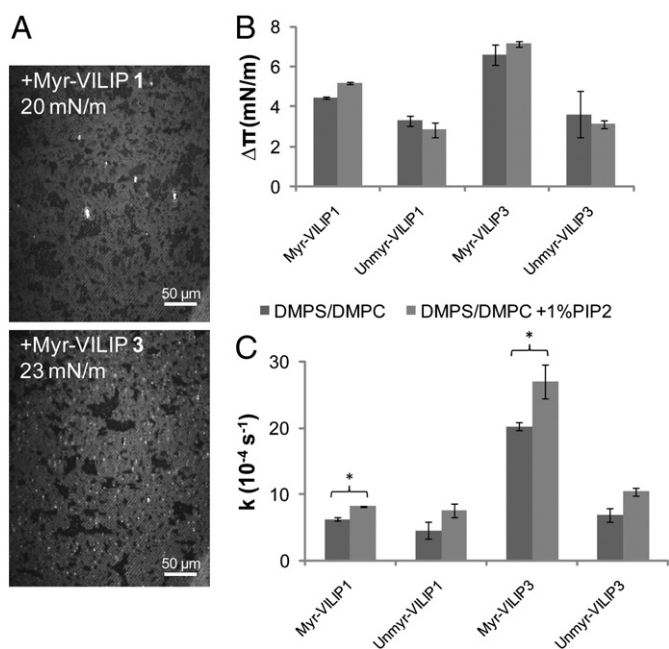

Fig. 6. Influence of PIP_2 on VILIPs membrane binding properties. (A) Interface visualization using Brewster angle microscopy of DMPC/DMPS (1:3) containing 1% PIP_2 at negative constant charge. (B) Surface pressure increase (ΔΠ) upon interaction of VILIPs injected under DMPC/DMPS (1:3) ± 1% PIP_2 monolayers in the presence of 2 mM calcium. (C) Rate of binding determined in the same experimental conditions (*p < 0.02).

In the presence of calcium, the association of myristoylated forms is markedly accelerated (highest k values), but at the end, the same final organization is reached (same $\Delta\pi$ values obtained for wild-type proteins in the presence or not of Ca^{2+}, Fig. 3). The presence of calcium affects the kinetics of binding of the proteins but not the final affinity. Again this result presents striking similarity with the finding of Strittmatter et al. who reported that the effect of N-myristoylation appears to be restricted to facilitate and stabilize the interaction of the cytochrome b5 reductase NADH with phospholipid vesicles [70].

Given that the same $\Delta\pi$ value is obtained in the absence and in the presence of calcium, one could postulate that the myristoyl group of the protein is extracted from its protein-buried location and inserted into the monolayer whatever the concentration of calcium is. This phenomenon is not observed if the lipids are not present at the air–liquid interface; on the contrary, the kinetics are not changed and the equilibrium surface pressure π_e is higher for the N-myristoylated proteins in the presence of calcium (Fig. 2).

Altogether, this result highlights a putative synergy between electrostatic interactions and N-myristoylation in the presence of calcium, for VILIP binding to membranes. As previously shown [46], electrostatic interactions are likely responsible for the very first interactions of the protein with the membrane. In the absence of calcium, once associated to the membrane, one could postulate that some conformational changes might operate to ensure the extrusion of the myristoyl moiety from its hydrophobic pocket and anchor the protein to the membrane, thus leading to no apparent change in the final affinity of N-myristoylated proteins. In the presence of calcium, the ejection is triggered and the insertion of the myristate within the membrane is faster, which only impacts the adsorption kinetics of the N-myristoylated proteins (not the final membrane-bound state). This kinetic role is consistent with the possible function of the N-myristoylated proteins regulated by a 'calcium–myristoyl switch' in the activation (or termination) of signaling process. Since in the absence of electrostatic interactions (interface without lipid), the myristoyl group does not eject if calcium is not present (Fig. 2), it may be also assumed that the electrostatic interactions prefigure the rapid conformational changes triggered by the calcium binding.

The analysis of the influence of the lipid packing on VILIP–membrane interaction has shown that N-myristoylated proteins exhibit a higher affinity than unmyristoylated forms as shown by the higher MIPs (Fig. 4). This result is consistent with the two-signal model 'myristate plus basic' in which the hydrophobic and electrostatic forces synergize to mediate efficient membrane binding: the positively charged residues associate electrostatically with acidic phospholipids to stabilize membrane binding, while myristate provides membrane-binding energy via hydrophobic interactions, giving a great binding ability to the wild-type proteins [9]. As revealed by the analysis of the synergy factor, the insertion of the myristoyl moiety within the monolayer is favored by the packing of the phospholipid acyl chains. (Membrane binding of VILIPs becomes insensitive to the acyl chain organization when it is only mediated by electrostatic interactions). Adding a myristate confers a relatively small hydrophobicity to the protein because this saturated acyl chain is short. If the penetration of the myristate into the membrane is favored by the packing chain, it is probably because the hydrophobic interactions are more stronger in a more condensed monolayer and this result in the stabilization of the myristate moiety in the membrane after insertion (approximately 10 of the 14 carbons penetrate the hydrocarbon core of bilayer [13]). This point may be correlated to the possible targeting of lipid-modified proteins to plasma membrane nanodomains, when a second acylation occurs [12].

BAM analysis of the morphology changes of a mixed monolayer of DMPC/DMPS (1:3) segregated by the presence of calcium in the subphase upon interaction of both N-myristoylated and non-myristoylated forms of VILIPs has clearly evidenced that VILIPs interact more specifically with phosphatidylserine (PS) (red arrows, Fig. 5). This result confirms that VILIPs can interact with acidic phospholipid headgroups. This

interaction could presumably be mediated by the conserved polybasic residues in the N-terminus [22]. But, more interesting is the specific effect of PIP_2 on the membrane binding of VILIPs. Adding only 1% of PIP_2 – which corresponds to the percentage of this phosphoinositide in the cytoplasmic leaflet of the plasma membrane [24,68] – to DMPC/DMPS mixture while maintaining constant the negative charge amount in the monolayer provokes an increase of the binding kinetics rate of all myristoylated and unmyristoylated proteins (higher rates of binding k, Fig. 6) without changing their final membrane-bound states (same $\Delta\pi$ values, Fig. 6). This phenomenon is probably the result of specific electrostatic interactions between the conserved polybasic domain and the highly charged PIP_2 headgroup [22] which reinforces the association of VILIPs to the membrane. In the case of N-myristoylated proteins, we can conclude that this tightening may assist the conformational changes triggered by the calcium binding. This effect is in perfect agreement with a PIP-dependent targeting mechanism that directs VILIPs to particular subcellular localization where it can promote distinct cellular processes [2].

In conclusion, all results obtained in this present report highlight the distinct role of electrostatic interactions which could presumably be mediated by the polybasic domain in the N-terminal region of VILIPs, and interaction of the myristoyl moiety with the membrane, which might be triggered by calcium binding. We propose that electrostatic interactions would be responsible for the very first interactions of the protein with the membrane, and the extrusion of the myristoyl group would have only an impact on the adsorption kinetic rates of the N-myristoylated proteins. Additionally, membrane interactions that would solely be mediated by electrostatic interactions would also presumably lead to an extrusion of the myristoyl moiety. In view of the present results, one could postulate that electrostatic interactions help to the efficiency of the calcium binding to the protein by inducing subtle conformational changes that would assist the binding of calcium that triggers the release of the myristoyl group. This point seems to be exemplified by the specific interactions with PIP_2. The specific electrostatic interactions with PIP_2 would be not simply requested for the first step of the membrane targeting: they could contribute also to an accelerated membrane binding process. This kinetic effect is consistent with the activation of subcellular signaling processes mediated by the specific interactions with PIPs of proteins which are addressed to the plasma membrane where they regulate the function of various membrane receptors.

References

[1] C. Spilker, T. Dresbach, K.H. Braunewell, Reversible translocation and activity-dependent localization of the calcium-myristoyl switch protein VILIP-1 to different membrane compartments in living hippocampal neurons, J. Neurosci. 22 (2002) 7331–7339.

[2] C. Spilker, K.H. Braunewell, Calcium–myristoyl switch, subcellular localization, and calcium-dependent translocation of the neuronal calcium sensor protein VILIP-3, and comparison with VILIP-1 in hippocampal neurons, Mol. Cell. Neurosci. 24 (2003) 766–778.

[3] C. Li, W. Pan, K.H. Braunewell, J.B. Ames, Structural analysis of Mg2 + and Ca2 + binding, myristoylation, and dimerization of the neuronal calcium sensor and visinin-like protein 1 (VILIP-1), J. Biol. Chem. 286 (2011) 6354–6366.

[4] S. Maurer-Stroh, B. Eisenhaber, F. Eisenhaber, N-terminal N-myristoylation of proteins: refinement of the sequence motif and its taxon-specific differences, J. Mol. Biol. 317 (2002) 523–540.

[5] T. Chida, M. Ando, T. Matsuki, Y. Masu, Y. Nagaura, T. Takano, S. Tamura Yamamoto, T. Kobayashi, N-Myristoylation is essential for protein phosphatases PPM1A and PPM1B to dephosphorylate their physiological substrates in cells, Biochem. J. 449 (2013) 741–749.

[6] D.D.O. Martin, E. Beauchamp, L.G. Berthiaume, Post-translational myristoylation: fat matters in cellular life and death, Biochimie 93 (2011) 18–31.

[7] M.D. Resh, Trafficking and signaling by fatty-acylated and prenylated proteins, Nat. Chem. Biol. 2 (2006) 584–590.

[8] M.D. Resh, Targeting protein lipidation in disease, Trends Mol. Med. 18 (2012) 206–214.

[9] M.D. Resh, Covalent lipid modifications of proteins, Curr. Biol. 23 (2013) R431–R435.

[10] H. Ezanno, E. Beauchamp, F. Lemarié, P. Legrand, V. Rioux, L'acylation des protéines: une fonction cellulaire importante des acides gras saturés, Nutr. Clin. Metab. 27 (2013) 10–19.

[11] N. Sorek, D. Bloch, S. Yalovsky, Protein lipid modifications in signaling and subcellular targeting, Curr. Opin. Plant Biol. 12 (2009) 714–720.

[12] J.A. Traverso, C. Micaelela, A. Martinez, S.C. Brown, B. Satiat-Jeunemaître, T. Meinnel, C. Giglione, Roles of N-terminal fatty acid acylations in membrane compartment partitioning: arabidopsis h-type thioredoxins as a case study, Plant Cell Online 25 (2013) 1056–1077.

[13] M.D. Resh, Fatty acylation of proteins: new insights into membrane targeting of myristoylated and palmitoylated proteins, Biochim. Biophys. Acta (BBA), Mol. Cell. Res. 1451 (1999) 1–16.

[14] S. Maurer-Stroh, F. Eisenhaber, Myristoylation of viral and bacterial proteins, Trends Microbiol. 12 (2004) 178–185.

[15] M. Wright, W. Heal, D. Mann, E. Tate, Protein myristoylation in health and disease, J. Chem. Biol. 3 (2010) 19–35.

[16] R.M. Peitzsch, S. McLaughlin, Binding of acylated peptides and fatty acids to phospholipid vesicles: pertinence to myristoylated proteins, Biochemistry 32 (1993) 10436–10443.

[17] M. Resh, Membrane targeting of lipid modified signal transduction proteins, in: P. Quinn (Ed.), Membrane Dynamics and Domains, vol. 37, Springer US, 2004, pp. 217–232.

[18] J.B. McCabe, L.G. Berthiaume, Functional roles for fatty acylated amino-terminal domains in subcellular localization, Mol. Biol. Cell 10 (1999) 3771–3786.

[19] R. Tarawneh, G. D'Angelo, E. Macy, C. Xiong, D. Carter, N.J. Cairns, A.M. Fagan, D. Head, M.A. Mintun, J.H. Ladenson, J.M. Lee, J.C. Morris, D.M. Holtzman, Visinin-like protein-1: diagnostic and prognostic biomarker in Alzheimer disease, Ann. Neurol. 70 (2011) 274–285.

[20] L.J. Parent, C.B. Wilson, M.D. Resh, J.W. Wills, Evidence for a second function of the MA sequence in the Rous sarcoma virus Gag protein, J. Virol. 70 (1996) 1016–1026.

[21] D.W. O'Callaghan, L.P. Haynes, R.D. Burgoyne, High-affinity interaction of the N-terminal myristoylation motif of the neuronal calcium sensor protein hippocalcin with phosphatidylinositol 4,5-bisphosphate, Biochem. J. 391 (2005) 231–238.

[22] K. Braunewell, B. Paul, W. Altarche-Xifro, C. Noack, K. Lange, A. Hofmann, Interactions of visinin-like proteins with phospho-inositides, Aust. J. Chem. 63 (2010) 350–356.

[23] S. McLaughlin, J. Wang, A. Gambhir, D. Murray, PIP2 AND PROTEINS: interactions, organization, and information flow, Annu. Rev. Biophys. Biomol. Struct. 31 (2002) 151–175.

[24] M.P. Czech, PIP2 and PIP3: complex roles at the cell surface, Cell 100 (2000) 603–606.

[25] W.D. Heo, T. Inoue, W.S. Park, M.L. Kim, B.O. Park, T.J. Wandless, T. Meyer, PI(3,4,5)P3 and PI(4,5)P2 lipids target proteins with polybasic clusters to the plasma membrane, Science 314 (2006) 1458–1461.

[26] J.B. Ames, T. Tanaka, L. Stryer, M. Ikura, Portrait of a myristoyl switch protein, Curr. Opin. Struct. Biol. 6 (1996) 432–438.

[27] J.B. Ames, R. Ishima, T. Tanaka, J.I. Gordon, L. Stryer, M. Ikura, Molecular mechanics of calcium–myristoyl switches, Nature 389 (1997) 198–202.

[28] S. McLaughlin, A. Aderem, The myristoyl-electrostatic switch: a modulator of reversible protein–membrane interactions, Trends Biochem. Sci. 20 (1995) 272–276.

[29] K.H. Braunewell, A.J. Klein-Szanto, Visinin-like proteins (VSNLs): interaction-partners and emerging functions in signal transduction of a subfamily of neuronal Ca^{2+} − sensor proteins, Cell Tissue Res. 335 (2009) 301–316.

[30] J.F. Loring, X. Wen, J.M. Lee, J. Seilhamer, R. Somogyi, A gene expression profile of Alzheimer's disease, DNA Cell Biol. 20 (2001) 683–695.

[31] X. Luo, L. Hou, H. Shi, X. Zhong, Y. Zhang, D. Zheng, Y. Tan, G. Hu, N. Mu, J. Chan, X. Chen, Y. Fang, F. Wu, H. He, Y. Ning, CSF levels of the neuronal injury biomarker visinin-like protein-1 in Alzheimer's disease and dementia with Lewy bodies, J. Neurochem. 127 (2013) 681–690.

[32] H.-G. Bernstein, K.-H. Braunewell, C. Spilker, P. Danos, B. Baumann, S. Funke, S. Diekmann, E.D. Gundelfinger, B. Bogerts, Hippocampal expression of the calcium sensor protein visinin-like protein-1 in schizophrenia, NeuroReport 13 (2002) 393–396.

[33] P. Gierke, C. Zhao, H.G. Bernstein, C. Noack, R. Anand, U. Heinemann, K.H. Braunewell, Implication of neuronal Ca2+-sensor protein VILIP-1 in the glutamate hypothesis of schizophrenia, Neurobiol. Dis. 32 (2008) 162–175.

[34] H. Mahloogi, A.M. Gonzalez-Guerrico, R. Lopez De Cicco, D.E. Bassi, T. Goodrow, K.H. Braunewell, A.J. Klein-Szanto, Overexpression of the calcium sensor visinin-like protein-1 leads to a cAMP-mediated decrease of in vivo and in vitro growth and invasiveness of squamous cell carcinoma cells, Cancer Res. 63 (2003) 4997–5004.

[35] J. Fu, K. Fong, A. Bellacosa, E. Ross, S. Apostolou, D.E. Bassi, F. Jin, J. Zhang, P. Cairns, I. Ibanez de Caceres, K.H. Braunewell, A.J. Klein-Szanto, VILIP-1 downregulation in non-small cell lung carcinomas: mechanisms and prediction of survival, PLoS One 3 (2008) e1698.

[36] M. Liu, H. Yang, D. Fang, J.J. Yang, J. Cai, Y. Wan, D.H. Chui, J.S. Han, G.G. Xing, Upregulation of P2X3 receptors by neuronal calcium sensor protein VILIP-1 in dorsal root ganglions contributes to the bone cancer pain in rats, Pain 154 (2013) 1551–1568.

[37] F.F. Dai, Y. Zhang, Y. Kang, Q. Wang, H.Y. Gaisano, K.H. Braunewell, C.B. Chan, M.B. Wheeler, The neuronal Ca2 + sensor protein visinin-like protein-1 is expressed in pancreatic islets and regulates insulin secretion, J. Biol. Chem. 281 (2006) 21942–21953.

[38] C.J. Zhao, C. Noack, M. Brackmann, T. Gloveli, A. Maelicke, U. Heinemann, R. Anand, K.H. Braunewell, Neuronal Ca2 + sensor VILIP-1 leads to the upregulation of functional alpha4beta2 nicotinic acetylcholine receptors in hippocampal neurons, Mol. Cell. Neurosci. 40 (2009) 280–292.

[39] J. Buttgereit, F. Qadri, J. Monti, T.H. Langenickel, R. Dietz, K.H. Braunewell, M. Bader, Visinin-like protein 1 regulates natriuretic peptide receptor B in the heart, Regul. Pept. 161 (2010) 51–57.

[40] C. Spilker, E.D. Gundelfinger, K.H. Braunewell, Evidence for different functional properties of the neuronal calcium sensor proteins VILIP-1 and VILIP-3: from subcellular localization to cellular function, Biochim. Biophys. Acta 4 (2002) 1–2.

[41] C.K. Wang, A. Simon, C.M. Jessen, C.L.P. Oliveira, L. Mack, K.-H. Braunewell, J.B. Ames, J.S. Pedersen, A. Hofmann, Divalent cations and redox conditions regulate the molecular structure and function of visinin-like protein-1, PLoS One 6 (2011) e26793.

[42] K.C. Chen, L.K. Wang, L.S. Chang, Regulatory elements and functional implication for the formation of dimeric visinin-like protein-1, J. Pept. Sci. 15 (2009) 89–94.

[43] T. Tanaka, J.B. Ames, T.S. Harvey, L. Stryer, M. Ikura, Sequestration of the membrane-targeting myristoyl group of recoverin in the calcium-free state, Nature 376 (1995) 444–447.

[44] P. Desmeules, S.-É. Penney, B. Desbat, C. Salesse, Determination of the contribution of the myristoyl group and hydrophobic amino acids of recoverin on its dynamics of binding to lipid monolayers, Biophys. J. 93 (2007) 2069–2082.

[45] J. Boucher, E. Trudel, M. Méthot, P. Desmeules, C. Salesse, Organization, structure and activity of proteins in monolayers, Colloids Surf. B: Biointerfaces 58 (2007) 73–90.

[46] S. Rebaud, A. Simon, C.K. Wang, L. Mason, L. Blum, A. Hofmann, A. Girard-Egrot, Comparison of VILIP-1 and VILIP-3 binding to phospholipid monolayers, PLoS One 9 (2014) e93948.

[47] E. Boisselier, P. Calvez, E. Demers, L. Cantin, C. Salesse, Effect of oxidation of polyunsaturated phospholipids on the binding of proteins in monolayers, Colloids Surf. B Biointerfaces 109 (2013) 109–114.

[48] J.A. Cox, I. Durussel, M. Comte, S. Nef, P. Nef, S.E. Lenz, E.D. Gundelfinger, Cation binding and conformational changes in VILIP and NCS-1, two neuron-specific calcium-binding proteins, J. Biol. Chem. 269 (1994) 32807–32813.

[49] W.H. Pitcher III, S.L. Keller, W.H. Huestis, Interaction of nominally soluble proteins with phospholipid monolayers at the air–water interface, Biochim. Biophys. Acta Biomembr. 1564 (2002) 107–113.

[50] P. Calvez, E. Demers, E. Boisselier, C. Salesse, Analysis of the contribution of saturated and polyunsaturated phospholipid monolayers to the binding of proteins, Langmuir 27 (2011) 1373–1379.

[51] É. Boisselier, P. Calvez, É. Demers, L. Cantin, C. Salesse, Influence of the physical state of phospholipid monolayers on protein binding, Langmuir 28 (2012) 9680–9688.

[52] D. Vollhardt, Morphology and phase behavior of monolayers, Adv. Colloid Interf. Sci. 64 (1996) 143–171.

[53] M.N.G. de Mul, J.A. Mann, Determination of the thickness and optical properties of a Langmuir film from the domain morphology by Brewster angle microscopy, Langmuir 14 (1998) 2455–2466.

[54] K. Winsel, D. Hönig, K. Lunkenheimer, K. Geggel, C. Witt, Quantitative Brewster angle microscopy of the surface film of human broncho-alveolar lavage fluid, Eur. Biophys. J. 32 (2003) 544–552.

[55] J. Saccani, S. Castano, F. Beaurain, M. Laguerre, B. Desbat, Stabilization of phospholipid multilayers at the air–water interface by Compression beyond the collapse: A BAM, PM-IRRAS, and molecular dynamics study, Langmuir 20 (2004) 9190–9197.

[56] A.l.A.M. Santafé, L.c.J. Blum, C.A. Marquette, A.s.P. Girard-Egrot, Chelating Langmuir–Blodgett film: a new versatile chemiluminescent sensing layer for biosensor applications, Langmuir 26 (2009) 2160–2166.

[57] H.P. Ta, K. Berthelot, B. Coulary-Salin, B. Desbat, J. Gean, L. Servant, C. Cullin, S. Lecomte, Comparative studies of nontoxic and toxic amyloids interacting with membrane models at the air–water interface, Langmuir 27 (2011) 4797–4807.

[58] O. Maniti, M.F. Lecompte, O. Marcillat, B. Desbat, R. Buchet, C. Vial, T. Granjon, Mitochondrial creatine kinase binding to phospholipid monolayers induces cardiolipin segregation, Biophys. J. 96 (2009) 2428–2438.

[59] J.M. Rodríguez Patino, C.C. Sánchez, M.R. Rodríguez Niño, Morphological and structural characteristics of monoglyceride monolayers at the air–water interface observed by Brewster angle microscopy, Langmuir 15 (1999) 2484–2492.

[60] Y. Guillemin, J. Lopez, D. Gimenez, G. Fuertes, J.G. Valero, L. Blum, P. Gonzalo, J. Salgado, A. Girard-Egrot, A. Aouacheria, Active fragments from pro- and antiapoptotic BCL-2 proteins have distinct membrane behavior reflecting their functional divergence, PLoS One 5 (2010) e9066.

[61] C. Larios, J. Miñones, I. Haro, M.A. Alsina, M.A. Busquets, J. Miñones Trillo, Study of adsorption and penetration of E2(279–298) peptide into Langmuir phospholipid monolayers, J. Phys. Chem. B 110 (2006) 23292–23299.

[62] J. Sarkis, J.F. Hubert, B. Legrand, E. Robert, A. Cheron, J. Jardin, E. Hitti, E. Le Rumeur, V. Vie, Spectrin-like repeats 11–15 of human dystrophin show adaptations to a lipidic environment, J. Biol. Chem. 286 (2011) 30481–30491.

[63] A. Girard-Egrot, J.-P. Chauvet, G. Gillet, M. Moradi-Améli, Specific interaction of the antiapoptotic protein Nr-13 with phospholipid monolayers is prevented by the BH3 domain of Bax, J. Mol. Biol. 335 (2004) 321–331.

[64] L. Francois-Moutal, O. Maniti, O. Marcillat, T. Granjon, New insights into lipid-nucleoside diphosphate kinase-D interaction mechanism: protein structural changes and membrane reorganisation, Biochim. Biophys. Acta Biomembr. 1828 (2013) 906–915.

[65] J. Sarkis, J. Rocha, O. Maniti, J. Jouhet, V. Vié, M.A. Block, C. Breton, E. Maréchal, A. Girard-Egrot, The influence of lipids on MGD1 membrane binding highlights novel mechanisms for galactolipid biosynthesis regulation in chloroplasts, FASEB J. 28 (2014) 3114–3123.

[66] S. Brot, C. Auger, R. Bentata, V. Rogemond, S. Ménigoz, N. Chounlamountri, A. Girard-Egrot, J. Honnorat, M. Moradi-Améli, Collapsin Response Mediator Protein 5 (CRMP5) induces mitophagy, thereby regulating mitochondrion numbers in dendrites, J. Biol. Chem. 289 (2014) 2261–2276.

[67] S. Redon, J. Massin, S. Pouvreau, E. De Meulenaere, K. Clays, Y. Queneau, C. Andraud, A. Girard-Egrot, Y. Bretonnière, S. Chambert, Red emitting neutral fluorescent glycoconjugates for membrane optical imaging, Bioconjug. Chem. 25 (2014) 773–787.

[68] S. McLaughlin, D. Murray, Plasma membrane phosphoinositide organization by protein electrostatics, Nature 438 (2005) 605–611.

[69] M.P. Liebl, A.M. Kaya, S. Tenzer, R. Mittenzwei, I. Koziollek-Drechsler, H. Schild, B. Moosmann, C. Behl, A.M. Clement, Dimerization of visinin-like protein 1 is regulated by oxidative stress and calcium and is a pathological hallmark of amyotrophic lateral sclerosis, Free Radic. Biol. Med. 72 (2014) 41–54.

[70] P. Strittmatter, J.M. Kittler, J.E. Coghill, J. Ozols, Interaction of non-myristoylated NADH-cytochrome b5 reductase with cytochrome b5-dimyristoylphosphatidylcholine vesicles, J. Biol. Chem. 268 (1993) 23168–23171.